Tobias Weidner*, Damir Druzinec, Martina Mühlmann, Rainer Buchholz and Peter Czermak

The components of shear stress affecting insect cells used with the baculovirus expression vector system

https://doi.org/10.1515/znc-2017-0066 Received April 18, 2017; revised July 3, 2017; accepted July 17, 2017

Abstract: Insect-based expression platforms such as the baculovirus expression vector system (BEVS) are widely used for the laboratory- and industrial-scale production of recombinant proteins. Thereby, major drawbacks to gain high-quality proteins are the lytic infection cycle and the shear sensitivity of infected insect cells due to turbulence and aeration. Smaller bubbles were formerly assumed to be more harmful than larger ones, but we found that cell damage is also dependent on the concentration of protective agents such as Pluronic®. At the appropriate concentration, Pluronic forms a layer around air bubbles and hinders the attachment of cells, thus limiting the damage. In this context, we used microaeration to vary bubble sizes and confirmed that size is not the most important factor, but the total gas surface area in the reactor is. If the surface area exceeds a certain threshold, the concentration of Pluronic is no longer sufficient for cell protection. To investigate the significance of shear forces, a second study was carried out in which infected insect cells were cultivated in a hollow fiber module to protect them from shear forces. Both model studies revealed important aspects of the design and scale-up of BEVS processes for the production of recombinant proteins.

*Corresponding author: Tobias Weidner, Institute of Bioprocess Engineering and Pharmaceutical Technology, University of Applied Sciences Mittelhessen, Giessen, Germany,

E-mail: tobias.weidner@lse.thm.de; and Institute of Bioprocess Engineering, Friedrich-Alexander University of Erlangen-Nuremberg, Erlangen, Germany

Damir Druzinec: Institute of Bioprocess Engineering and Pharmaceutical Technology, University of Applied Sciences Mittelhessen, Giessen, Germany

Martina Mühlmann and Rainer Buchholz: Institute of Bioprocess Engineering, Friedrich-Alexander University of Erlangen-Nuremberg, Erlangen, Germany

Peter Czermak: Institute of Bioprocess Engineering and Pharmaceutical Technology, University of Applied Sciences Mittelhessen, Giessen, Germany; Department of Chemical Engineering, Kansas State University, Manhattan, KS, USA; and Fraunhofer Institute for Molecular Biology and Applied Ecology, Project Group Bioresources, Giessen, Germany **Keywords:** baculovirus expression vector system; Pluronic[®]; shear stress; Sf-21 cells.

1 Introduction

The establishment of the first stable insect cell line in the 1960s led to the development of more than 500 different cell lines that are still used today [1, 2]. More than 300 of these cell lines are derived from lepidopteran species [3]. The use of insect cells as an expression system for recombinant proteins began with the production of human interferon β using insect cells infected with a recombinant baculovirus expression vector [4]. Today, the most popular insect cell lines for protein expression are derived from Spodoptera frugiperda (Sf9 and Sf21), Trichoplusia ni (High Five™) and *Drosophila melanogaster* (S2). Recombinant protein production in S2 cells is achieved by stable transformation [5–7]. The other cell lines are used to host the baculovirus expression vector system (BEVS), which remains the gold standard in insect-based expression systems for recombinant proteins [8, 9]. However, the BEVS is used not only for the production of recombinant proteins but also as a gene shuttle for stem cells [10] and for vaccine manufacturing [9].

The production of recombinant proteins using the BEVS involves a multistage process in which cell growth is followed by virus infection. The early infection phase involves virus replication and secretion, whereas the recombinant protein is typically expressed under the control of a promoter that becomes active later in the infection cycle. Depending on the genetic construct, the recombinant protein can accumulate in the cell or can be secreted into the medium. During the infection, the virus takes complete control of the host cell, increasing its catabolic metabolism and thus causing higher oxygen consumption [11, 12]. The infected cells are arrested in the G2/M phase [13] and cytoskeleton is destabilized [14, 15]. The accumulation of virus protein causes the host cell to swell, increasing its diameter by 40%-50% and ultimately perforating the membrane to release virus particles and recombinant protein into the medium [16].

The complex events described previously and the effect of the virus on cell metabolism poses some unusual demands in terms of cultivation conditions, particularly the higher oxygen demand and the lytic infection cycle. Compared with mammalian cell lines, such as Chinese hamster ovary (CHO) cells with an oxygen uptake rate (qO_2) of $6.9-9.7\times10^{-17}$ mol·cell⁻¹·s⁻¹ [17, 18], hybridomas (4.2– 13×10^{-17} mol·cell⁻¹·s⁻¹) [19, 20], and NS0 cells (6.1–11×10⁻¹⁷ mol·cell⁻¹·s⁻¹) [21], baculovirus-infected Sf9 cells consume significantly more oxygen (8.6–26×10⁻¹⁷ mol·cell⁻¹·s⁻¹) [22– 24]. As well as addressing the higher oxygen demand, a BEVS process must also deal with the increased sensitivity of the cells to shear stress caused by the loss of repair mechanisms as the cells swell and burst. Gentle cultivation conditions are therefore required to avoid shear stress and maintain cell viability for as long as possible, thus increasing the yield of recombinant protein. Several reactor systems with low shear stress and high rates of oxygen and carbon dioxide transfer have been designed or adapted for the BEVS, including the rotating wall reactor [25] and the wave reactor [26]. However, most processes still use a stirred-tank reactor (STR) due to the simpler process control and scalability [27, 28].

1.1 Stirring-related shear stress

The flow regime in a bioreactor originates from the three-dimensional overlay of eddies. The macroscopic eddies are formed directly by the stirrer. In a cascade-like manner, the macroscopic eddies collapse into smaller ones, thereby transferring and conserving the kinetic energy. As this process continues to the smallest stable eddies, the energy is dissipated into heat due to the viscosity of the fluid. The scale η of the eddies is dependent on the energy dissipation per mass (ε) and the viscosity (ν) of the fluid [29, 30]:

$$\eta = \left(\frac{\nu^3}{\overline{\varepsilon}}\right)^{\frac{1}{4}} \tag{1}$$

Because the field of shear stress is equal to the gradient field of fluid velocity, particles or cells approximately the same size as the eddies experience the greatest shear stress [31]. Larger eddies result in the convective motion of particles in the turbulent field.

However, in stirred tank bioreactors, a steep gradient in turbulence and resulting shear stress can be expected. Instead of regarding the average energy input, it may be a better approach to use the maximum energy dissipation at the stirrer tip for estimating the relevant eddy size. Introducing the stirrer tip speed w, the diameter of the stirrer $d_{\rm st}$ and a stirrer-specific dissipation coefficient $C_{\rm D}$, the maximum energy input $\varepsilon_{\rm max}$ can be calculated as follows [32]:

$$\varepsilon_{\text{max}} = C_{\text{D}} \cdot \frac{w_{\text{tip}}^3}{d_{\text{st}}} \tag{2}$$

Thus, the ratio $\frac{\eta}{d_c}$ of the eddy scale η and the diameter of the suspended cell d_c represents the probability for imposing stirrer-induced shear stress on the cell [33].

1.2 Aeration-related shear stress

In terms of cellular shear stress, the energy dissipation caused by aeration is often more severe than that caused by stirring. Bubble generation at the sparger, followed by the bubbles rising through the medium and breaking at the surface, causes a first order kinetic of cell damage [34]:

$$\frac{dX}{dt} = -k_{\rm d} \cdot X \tag{3}$$

Here, X represents the biomass concentration and $k_{\rm d}$ the specific death rate. The deactivation of insect cells in a bubble column can be used to determine the mechanistic of $k_{\rm d}$:

$$k_{\rm d} = \frac{24 \cdot Q \cdot V_{\rm K}}{\pi^2 \cdot d_{\rm p}^3 \cdot d_{\rm p}^2 \cdot h_{\rm r}} \tag{4}$$

Thus, the extent of cell death is proportional to the aeration rate Q and the specific volume in the wake of rising bubbles $V_{\rm K}$, and is inversely proportional to the diameter of the reactor $d_{\rm R}$, the height of fluid $h_{\rm L}$ and the bubble diameter $d_{\rm B}$ [35, 36]. In this context, bubble rupture is the event with the most effect on cell viability. Therefore, bubble diameter is the most important parameter because the acceleration of the fluid film during bubble rupture varies with the diameter. Small bubbles of, e.g. 1 mm diameter cause local peaks in fluid film velocity (6.4 m·s⁻¹) whereas the peaks decline with larger bubbles, e.g. bubbles of 6 mm diameter cause peaks of 0.94 m·s⁻¹ [37].

1.3 Protective agents

To overcome the cell damage that occurs in aerated STRs, most cultivation media contain protective agents such as methylcellulose, poly(ethylene glycol), or Pluronic®

F68. The protective effect may be physical, physiological, or a combination of both [34]. The most commonly used agent is Pluronic, a block copolymer consisting of poly(oxyethylene) and poly(oxypropylene), typically at concentrations of 0.5-3 g·L⁻¹. The main protective mechanism of Pluronic is the inhibition of cell adhesion to air bubbles [38, 39]. Further effects include the stabilization of cells by reducing the fluidity of the plasma membrane, and the stabilization of the gas-liquid interface, which slows down bubble rupture and dampens the corresponding velocity gradients [34].

Video microscopy has shown that cells cultivated without additives tend to attach to rising bubbles [40, 41]. The inclusion of 1 g·L⁻¹ Pluronic prevents this and therefore limits the resulting damage [42]. The efficiency of protection strongly depends on the bubble size, the concentration of Pluronic, and the cell density [43].

1.4 Consequences in practical applications

Although the cell damage caused by shear forces is well understood, it is not yet possible to design a scalable process that avoids shear forces completely while achieving other necessary cultivation parameters such as mixing time and aeration. Bioreactors are available with microspargers for oxygen-intensive processes such as the BEVS [44]. Especially for single-used solutions, microaeration is attractive, as the oxygenation can be operated in a pulsed manner [45, 46].

The high surface-to-volume ratio of the microbubbles significantly increases oxygen transfer into the medium especially when using oxygen-enriched air. Continuous aeration may therefore be unnecessary and can be replaced with controlled pulses that reduce foam formation and shear stress from the microbubbles. Protective additives such as Pluronic can reduce the damaging effects of bubbles even further [47].

Nevertheless, the interaction between cells and microbubbles in cultivation media remains incompletely understood. The behavior of microbubbles in a cell-free system under normal cultivation conditions has been investigated in a previous study, revealing that variations in bubble size are determined by coalescence in media containing Pluronic, such that the bubble size increases with the specific power input [48]. Here, we investigated the effects of energy input and simultaneous microsparging on the cultivation of insect cells infected with recombinant baculovirus. This effect was evaluated by comparing the results with a model cultivation of the same cells in a shaker flask applying low shear forces and hollow fiber module (HFM) to completely avoid shear stress.

2 Materials and methods

2.1 Insect cells and baculovirus

The model system for recombinant baculovirus expression used in this study was the S. frugiperda cell line Sf21 (Invitrogen, Germany) and a recombinant Autographa californica multiple nucleopolyhedrovirus (AcMNPV) carrying a green fluorescent protein (GFP) fusion gene. The virus concentration was measured as the 50% tissue culture infective dose (TCID₅₀) and presented in plaqueforming units (pfu) as previously described [49]. We maintained the virus in the concentration range $1-5\times10^8$ pfu. The preculture was kept in an exponential growth phase at 28 °C in a shaking flask under humidified atmosphere at 50 rpm. The cultivation in shaker flasks was kept in the same conditions. The cells were grown in serum-free medium (Excell 420, Sigma, USA or SF-900II, Thermo Fisher Scientific, USA) containing Pluronic. Both media achieved a constant growth rate of 0.8 ± 0.03 d⁻¹. The viable cell count was determined by trypan blue exclusion in triplicate.

2.2 Cultivation conditions for the evaluation of shear stress

Shear stress experiments were carried out in a 3-L glass bioreactor (Applikon, Netherlands) as single experiments. The baffled vessel (d=130 mm, $h_v=250$ mm) was filled with 1615 mL of SF-900 II medium and equipped with a sintered microsparger with a 15-um pore size (Applikon), located under the stirrer. This design accommodates various stirrer configurations, and we used a six-blade Rushton impeller with a diameter of 60 mm (Applikon) and a $3\times45^{\circ}$ (d=74 mm) pitched blade impeller (Applikon) resulting in downward pumping. The experiments were conducted with a turbulent flow regime. The power numbers for the stirrers were Ne=4 and Ne=2.3, respectively. The different stirrers were used to keep the energy input constant while varying the bubble size. The size and behavior of the gas bubbles during cultivation were monitored with in situ particle vision and measurement technology (Mettler-Toledo, Switzerland) using the setup, measurement principles, and analytical method described elsewhere [48]. Instead of probe dummies as

used previously, the reactor was equipped with and controlled by oxygen and pH sensors (Applisense, Netherlands). The vessel was inoculated with 1×10^6 cells·mL⁻¹ from the exponential preculture. To study the infected cells, the recombinant virus was added with a multiplicity of infection (MOI) of 0.01. During cultivation, the aeration rate was maintained at a constant 0.01 vvm.

The concentration of the GFP fusion protein was determined using a sandwich enzyme-linked immunosorbent assay. The protein in the culture supernatant was bound to GFP-Trap® 96-well plates (Chromotek, Germany) and detected using the GFP-specific antibody 3E5 (Chromotek) and a horseradish peroxidase-conjugated AffniPure goat anti-rat detection antibody (Jackson ImmunoResearch, USA). The samples were measured in triplicate.

2.3 Immobilization of insect cells to protect them against shear stress

Sf21 cells were cultivated in a shear-protected environment using a 15-cm HFM with a total surface area of 3000 cm² (FiberCell® Systems, USA) as single experiments. The HFM contained 4600 polysulfone fibers, each with a cutoff of 20 kDa (50%). The cells were retained in the 20-mL extra-capillary space (ECS). The HFM was continuously perfused through the capillaries in a medium loop, with an aerated and temperature-controlled (27 °C) peripheral STR (BioFlo 110, Eppendorf AG, Germany) as a medium reservoir (800 mL) equipped with pH and O₃ sensors. The cell concentration was assessed by measuring the oxygen consumption in the HFM using an optical sensor (Presens, Germany) upstream and downstream of the reactor. The calculations were based on a cell-specific oxygen consumption rate of 17.5×10^{-17} mol·cell⁻¹·s⁻¹ [50], and the residence time of the medium in the reactor was determined by the pump rate. The cell concentrations were calculated at stable plateaus in the oxygen consumption graph.

To prepare for cultivation, the HFM was rinsed with 2 mL ethanol, then 2 mL ultrapure water per square centimeter of membrane area, according to the manufacturer's specifications. The ECS was inoculated with 5×10^7 exponentially growing cells (corresponding to 2.5×10^5 cells·mL⁻¹) and the cells were distributed evenly in the module by flushing several times with two syringes adapted to the ECS ports. For protein expression, the preculture was mixed with the appropriate quantity of infected cells.

To ensure the spreading of the infection in the otherwise not actively mixed HFM, the ECS was flushed gently every day using two syringes. The infection was verified by

measuring GFP expression by flow cytometry using a BD LSR I device (Becton Dickinson, Germany). The proportion of infected cells was determined in the same manner later in the process. The lactate concentration in the medium reservoir was measured in triplicate using K-LATE assay according to the manufacturer's instructions (Megazyme, Ireland).

3 Results and discussion

3.1 Exemplary standard process for using the BEVS

The simplest setup to apply BEVS at the laboratory scale is the cultivation of cells in shaker flasks. In this bubble-free cultivation system, the oxygen supply solely occurs by diffusion. A gentle shaking is provided, and the kinetics of cell growth and the respective lysis following the infection can be studied under low shear environment. An exemplary process in shaker flasks is displayed in Figure 1. The uninfected culture proliferates exponentially for 3 days until the medium is spent and the cell concentration and the viability decline. Applying a MOI of 0.01, the cell growth is stopped due to the secondary infection 24 h postinfection. The viability starts to decrease after 3 days. A nearly synchronous infection of the cell culture (MOI 10) accelerates this process. Thus, within 4 days postinfection, the viability decreases to 40% [51].

To gain a measure of the conditions in the shaker flask, the average energy input can be calculated empirically [52, 53]:

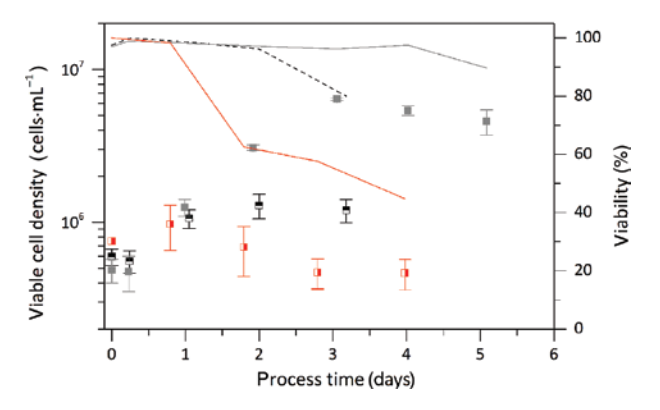


Figure 1: Cultivation of Sf21 in shaker flasks. Illustration of cell concentration and viability of an uninfected control culture (___, ___) as well as infected cultures using MOI 0.01 (___, - - -) and MOI 10 (___, - __).

$$\overline{\varepsilon} = Ne' \cdot n^3 \cdot d_{\rm sh}^4 \cdot V_{\rm L}^{-\frac{2}{3}} \tag{5}$$

Here, n represents the shaking frequency, d_{sh} the diameter of the shaker flask (8.9 cm), V_{τ} the volume of the medium (30 mL) and Ne' the modified power number, which can be described by the Reynolds number

$$Ne' = 75 \cdot Re^{-1} + 25 \cdot Re^{-0.6} + 1.5 \cdot Re^{-0.2}$$
 (6)

which is calculated using the viscosity v

$$Re = \frac{n \cdot d_{\rm sh}^2}{v}$$

Therefore, the average energy input was determined to 0.0139 W · kg⁻¹.

3.2 Effect of microbubble size on the viability of infected insect cells

Several theories have been proposed to explain the mechanisms of cell damage caused by stirring and aeration, but it is difficult to isolate the specific effects of varying the energy input from these sources because changing the energy input of the stirrer usually affects the bubble size too. Using different stirrer configurations, we separated these effects and used the ratio of the scale of the result- $\left| \frac{\eta}{d} \right|$ to estimate the shear stress ing eddies to the cell size

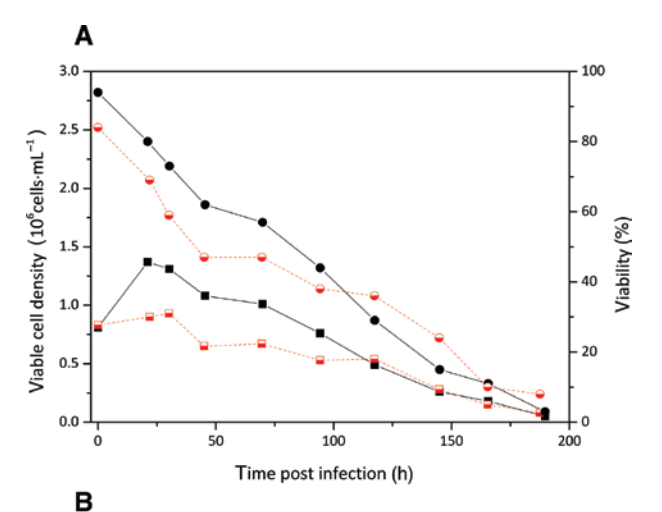
induced by the stirrer while varying the bubble size.

Because insect cells are more prone to shear stress after virus infection, the BEVS provides a good model to study the effect of both parameters on cell viability. As stated previously, insect cells can swell by up to 50% during infection, increasing from a typical diameter of 15 μm to a maximum diameter of 23 μm [16]. Using a relatively low MOI (0.01), we can assure that a full infection is delayed for at least 24 h. This allows to study the effect of the imposed shear forces for the first 24 h on a population of only approximately 1% infected cells [51]. Every effect seen in this time span would also be harmful to an uninfected culture. As demonstrated in Figure 1, a higher MOI (e.g. 10) causes almost total infection and therefore instantly affects the cells, the effect of the shear forces would be overlaid by the induced cell lyses.

In a first experiment (Figure 2), baculovirus-infected Sf21 cells were maintained under constant shear stress

$$\left(\frac{\eta}{d_{\rm c}}\!=\!1.1\right)$$
 whereas the bubble size distributions were

varied (mean diameter d_{32} =199 µm and d_{32} =208 µm). Under both conditions, the viable cell count decreased



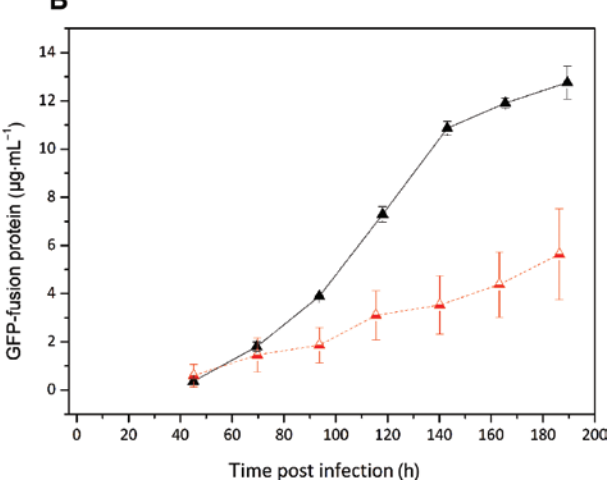


Figure 2: Changes in viable Sf21 cell density and viability (A) and the concentration of the GFP fusion protein (B) over the duration of

a process with a constant shear stress
$$\left(\frac{\eta}{d_{\rm c}}\!=\!$$
 1.1 $\right)$. The inoculum

of 1×106 cells · mL⁻¹ was infected at a MOI of 0.01 pfu·cell⁻¹, the aeration rate was maintained at 0.01 vvm and the concentration of dissolved oxygen (dO_3) was maintained at 70%. The graphs show the cell concentration ■, viability ●, and the concentration of the GFP fusion protein ▲ when aeration was performed with bubble sizes of $d_{32} = 199 \,\mu\text{m}$. The corresponding symbols =, =, and = refer to aeration with bubble sizes of $d_{32} = 208 \,\mu\text{m}$.

following virus infection as anticipated [24]. The decline was linear, with a viable cell count of >80% at the time of infection decreasing to <10% at ~200 h postinfection. Despite the assumption that smaller bubbles are more harmful [34], the maximum cell density was 34% higher (1.4×10⁶ cells⋅mL⁻¹) when the cells were exposed to the smaller bubbles (d_{32} =199 µm) compared with 0.9×10⁶ cells·mL⁻¹ when the cells were exposed to the larger bubbles (d_{xy} =208 µm). Exposure to the smaller bubbles also resulted in a larger proportion of viable cells and a 100% higher yield of the GFP fusion protein, confirming that the smaller bubbles were less harmful.

One possible interpretation of this phenomenon concerns the oxygen transfer coefficient ($k_{\rm La}$). Due to the different stirrer configurations, the $k_{\rm La}$ values for the smaller and larger bubbles were $9.53\pm0.23~{\rm h^{-1}}$ and $14.76\pm0.27~{\rm h^{-1}}$, respectively. Neither configuration therefore leads to oxygen transfer limitation. However, the ratio between $k_{\rm La}$ and the transport coefficient in the liquid ($k_{\rm L}$) can be used to calculate the specific area of the gas phase (a) [48]:

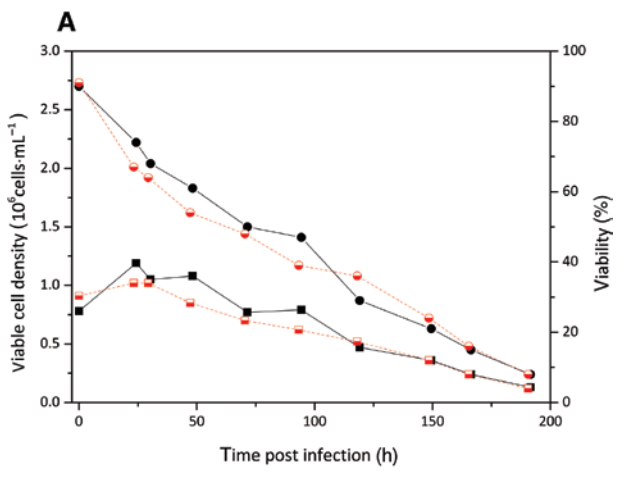
$$a = \frac{k_{\text{La}}}{k_{\text{r}}} \tag{7}$$

Here, $a = 12.28 \pm 0.38 \,\mathrm{m}^2 \cdot \mathrm{m}^{-3}$ for the smaller bubbles and $a=14.33\pm0.33$ m²·m⁻³ for the larger bubbles. The thickness of the liquid layer around air bubbles, which prevents the adsorption of cells to the bubbles and the consequential cell damage as the bubbles rise and rupture, is dependent on the concentration of Pluronic [43]. By reducing the concentration of Pluronic from a starting point of 0.1 g·L⁻¹, the liquid layer around the bubbles declined from ~40 µm to 16-20 µm, causing more cells to adhere to the bubbles and thus increasing the damage [43]. We found that increasing the bubble diameter led to an increase in the specific gas phase area, so more Pluronic was needed to stabilize the protective layer. Because the damage was more severe when cells were exposed to larger bubbles, the unbound or free concentration of the additive in the SF-900 II medium in the bulk of the fluid can be reduced. Below a certain layer thickness, more infected Sf21 cells are prone to adhere to the bubbles. This effect is a function of the total specific area of the gas phase and thus independent of the bubble diameter.

3.3 Varying the turbulence induced by stirring affects the viability of infected insect cells

Next, the effect of different stirring speeds was investigated to gain more insight into the mechanisms of cell damage in a turbulent microsparged system. Accordingly, the energy input was varied in addition to the bubble size (Figure 3). We observed slightly higher cell density $(1.05\times10^6$ and 1.2×10^6) and viability for the conditions

with higher energy input ($\frac{\eta}{d_c}$ = 0.85 and a bubble size of $d_{_{32}}$ = 208 µm), but no significant difference with an energy input of $\frac{\eta}{d_c}$ = 1.47 and a bubble diameter of $d_{_{32}}$ = 199 µm.



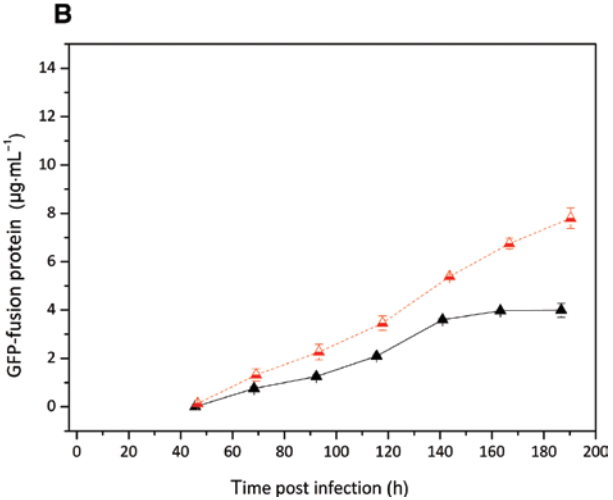


Figure 3: Changes in viable Sf21 cell density and viability (A) and the concentration of the GFP fusion protein (B) over the duration of a process in which the shear stress was varied using different stirrers and bubble sizes for aeration. The inoculum of 1×10^6 cells·mL⁻¹ was infected at a MOI of 0.01 pfu·cell⁻¹, the aeration rate was maintained at 0.01 vvm, and the concentration of dissolved oxygen (dO_2) was maintained at 70%. The graph shows the cell concentration \blacksquare , viability \blacksquare , and the concentration of GFP fusion protein \blacktriangle at aeration with an energy input of $\frac{\eta}{d_c} = 1.47$ (bubble size of $d_{32} = 199$ µm). The corresponding symbols \blacksquare , \blacksquare , and \blacktriangle refer to aeration with an energy input of $\frac{\eta}{d_c} = 0.85$ (bubble size of $d_{32} = 208$ µm).

However, when the energy input was increased, there was an unexpected ~100% increase in the yield of the GFP fusion protein. The specific area of the gas phase was $a=10.3\pm0.3$ m²·m³ for the higher energy input $(\frac{\eta}{d_c}=0.85)$ and $a=18.0\pm0.4$ m²·m³ for the lower energy input $(\frac{\eta}{d_c}=1.47)$. Thus, the observed behavior can also be explained by the depletion of Pluronic in the culture medium and a resulting increase in shear stress, despite

Table 1: Overview of the parameter setup in the STR case studies.

Case	Impeller	rpm (s ⁻¹)	Energy input (W·kg ⁻¹)	$\frac{\eta}{d_c}$	Bubble size d ₃₂ (μm)	Bubble surface to volume (m²·m³)	GFP yield (μg·mL⁻¹)
Figure 3	3×45° pitched blade	171	0.076	1.47	199	18.0	4.0
Figure 2	$3 \times 45^{\circ}$ pitched blade	250	0.24	1.10	208	14.33	5.6
Figure 3 ■	Six-blade Rushton	300	0.24	0.85	208	10.30	7.8
Figure 2 ■	Six-blade Rushton	205	0.076	1.10	199	12.28	12.75

Information on the used impeller, rpm, the resulting average energy input, ratio of eddy size and cell diameter, bubble size, total bubble to surface volume, and determined yield of GFP.

the milder cultivation conditions. For a better overview, the data and parameters for both STR cultivations are listed in Table 1.

The conditions of the previously introduced cultivation systems (STR and shaker flasks) cannot be directly compared. However, in the shaker flask, no direct aeration was applied and the introduced average shear forces (0.0139 W·kg⁻¹) were significantly lower compared with the STR (0.076 and 0.24 W·kg⁻¹). Thus, regarding the trend in cell concentration and viability, some conclusions can be drawn. In the shaker flask, there is no significant deviation in cell growth for the first 24 h when a MOI of 0.01 is applied (Figure 1). Cultivating the cells under the selected STR conditions, initial growth can only be observed when using the six-blade Rushton impeller for the experiments at both selected energy inputs. Also, independently of the setup, there is no apparent subsequent stagnation phase but the cell viability decreases constantly over the process time. These observations conclude that the conditions using the 3×45° pitched blade impeller, generating a higher specific area of gas phase, are more harmful to the cells and affects uninfected cells as well as infected cells.

3.4 BVES in shear-free environment

Although it is possible to distinguish the damage caused by aeration and stirring in the STR, it is not possible to evaluate the behavior of cells in an environment without shear stress using this type of bioreactor. We therefore cultivated uninfected and infected insect cell populations in a constantly perfused HFM. The viable cell concentration was calculated based on the oxygen consumption. During the first 8 days of cultivating the uninfected cells, a distinct growth-associated increase in oxygen demand was observed and approached with increasing the pump rate (Figure 4). There were some discontinuities, caused either by increasing the pump rate supplying

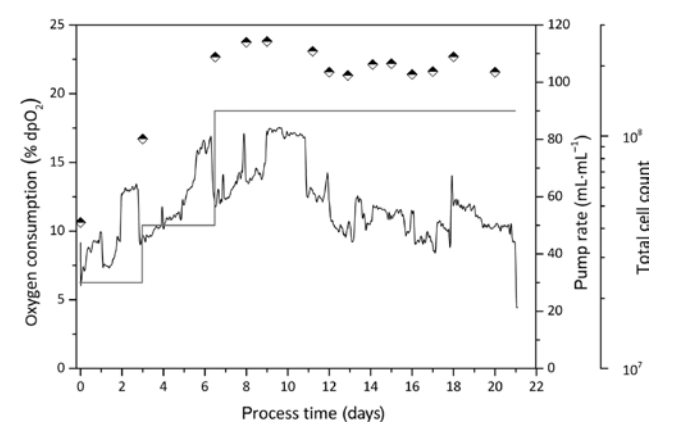


Figure 4: Total Sf21 cell density plotted against process time ♦ in an HFM. The cell density was calculated using the oxygen consumption and the pump rate —. The medium was aerated in the medium reservoir. The inoculum contained 5×10^7 not infected cells.

more oxygen to the cells, or by the interruption of perfusion when samples were taken. In this context, the initial pump rate of 30 mL·min-1 was increased to 50 and finally 90 mL·min⁻¹ after 3 and 7 days of cultivation. Even at the highest pump rate, the oxygen consumption remained at a plateau at about 17% before decreasing to a level at approximately 13%. Within the first 8 days, the inoculum of 5×10⁷ cells had expanded to a maximum total cell count of 2.55×108 corresponding to a concentration of about 1.3×10⁷ cells·mL⁻¹. This represents a growth rate of 0.25 d⁻¹, which is lower than the growth rate in the shaker experiments and preculture (0.8 ± 0.03 d-1) and in other studies using shaker flasks, STRs, or wave reactors (0.67-0.79 d⁻¹) [54-56].

For the evaluation of infected cells, the same setup was used with the supplementation of 1% infected cells in the initial inoculum (Figure 5). The graph of the oxygen consumption showed similar discontinuities than before. Here, the initial pump rate of 30 mL·min⁻¹ was increased to 50, 60, and finally 90 mL·min⁻¹ after 2, 5, and 13 days, respectively. Comparing the trend with the uninfected

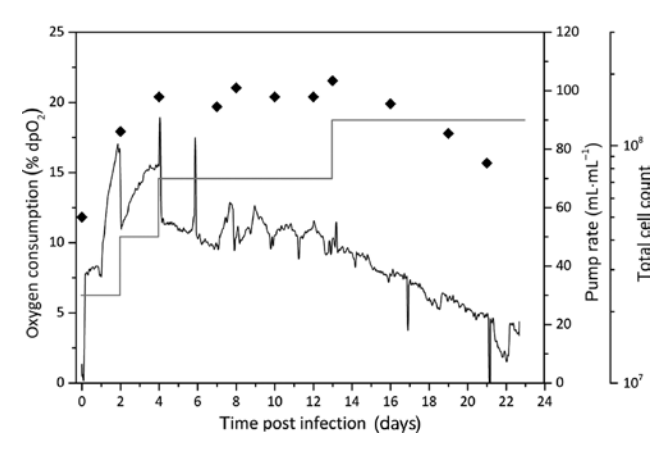


Figure 5: Total Sf21 cell density plotted against process time containing 1% infected cells \blacklozenge in a HFM. The cell density was calculated using the oxygen consumption —— and the pump rate ——. The medium was aerated in the medium reservoir. The inoculum of 5×10^7 cells contained 1% infected cells.

control culture, a steeper increase of the oxygen demand was observed during the first 5 days of cultivation. Afterward, the oxygen consumption remains more or less constant at a maximum total cell count of $2\times 10^8~(1\times 10^7~{\rm cells\cdot mL^{-1}})$ before a decline in cell concentration 16 days postinfection (1×10 7 cells·mL $^{-1}$). Compared with the uninfected culture, this results in a slightly higher growth rate of 0.29 d $^{-1}$.

Although few comparative studies have been reported, the most straightforward explanation for the slower growth rate is the formation of nutrient and oxygen gradients along the length of the HFM. The cells are supplied with nutrients by diffusion, so local limitations in the nutrient and oxygen supply may influence the cell growth and the overall oxygen consumption [57].

These assumed limitations would in turn have an effect on the metabolism of the insect cells. Thus, the cells are known to produce significant amounts of lactate when suffering oxygen limitation [12]. Here, lactate formation can be detected in both the uninfected and the infected HFM cultures (Figure 6). Thereby, the increase of the lactate concentration starts simultaneous with reaching the maximal cell density at the end of the exponential growth phase. Afterward, a nearly constant increase of the lactate concentration to approximately 12 mM and 10 mM was detected in the uninfected and infected culture, respectively. The observed behavior suggests that the oxygen transfer is the limiting factor concerning the maximal cell density. However, this fact does not explain the significantly decreased growth rate in the HFM compared with other systems. The reduced cell growth may be explained by the cell density effect.

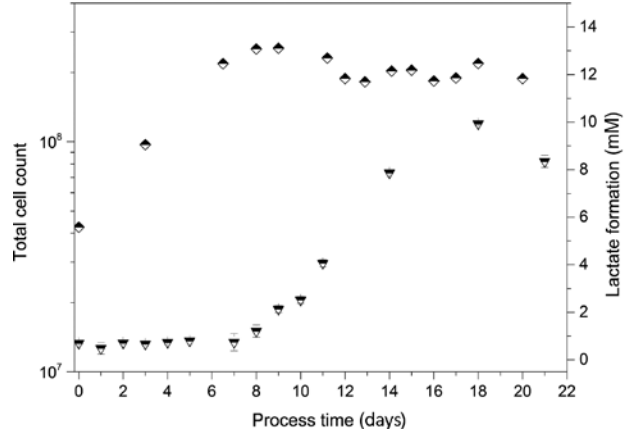


Figure 6: Lactate formation during the HFM cultivation. The graph shows the total cell count and resulting lactate formation for a culture with an inoculum of 5×10^7 not infected cells (\diamondsuit and \blacktriangledown) and a culture with an inoculum of 5×10^7 cells, containing 1% infected cells (\diamondsuit and \blacktriangledown).

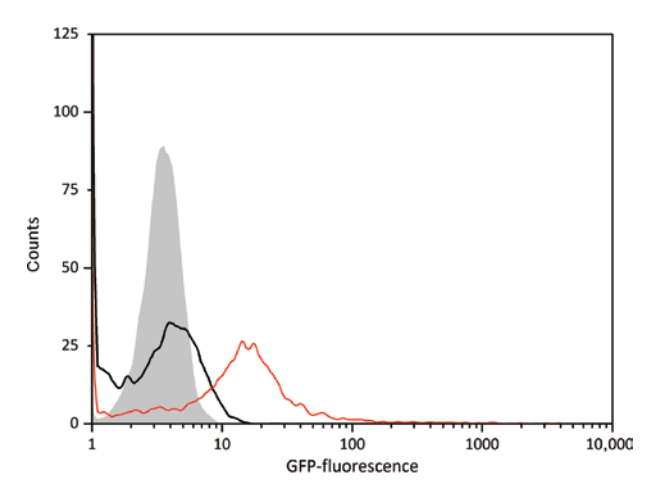


Figure 7: Determination of the ratio of infected cells using GFP expression and flow cytometry. The graph shows the negative, uninfected control and the infected cell population on day 1—and day 14—postinfection.

According to this phenomenon, the metabolism of the insect cells is downregulated, when the cells are kept at high density [12, 58].

During cultivation, the spreading of the infection within the cell population was monitored (Figure 7) using flow cytometry. Compared with the autofluorescence of the uninfected negative control, the ratio of infected cells increased from initially 1% to more than 70% on day 14 postinfection.

Thus, instead of the propagated lytic cycle of the baculovirus, which usually lasts until 72 h postinfection [27, 59, 60], longer cultivation periods are possible if shear stress is avoided.

specific area of the gas phase

4 Conclusion

Aeration with smaller (<2 mm) gas bubbles was proposed to generate high shear stress and cause extensive cell damage, especially during surface burst. The generated data show that Pluronic can dampen these effects, but that the protective effect is directly linked to the concentration of free Pluronic in the medium. By varying the stirrer type and thus the bubble size and energy input, we showed that increasing the overall surface area of the gas bubbles may exhaust the Pluronic, thus shrinking the protective layer around the bubbles and increasing the harmful effect of shear forces. Particularly regarding the cell viability in comparison to systems without direct aeration that reflects this effect. However, before giving practical instructions to optimize the conditions concerning the interdependency between shear stress and Pluronic concentration, more data should be gathered to gain a deeper understanding on the observed effect.

We also compared the STR environment to a HFM to avoid shear stress, and found that the BEVS process could be prolonged due to the physical protection of the cells. These results suggest that the lytic cycle in the BEVS reflects the effect of multiple and interconnected factors.

The scalability and productivity of BEVS processes therefore depends on several factors including the lytic cycle, which involves the release of proteases, the higher nutrient and oxygen demand of the infected insect cells, and the shear sensitivity of those cells. These factors are interlinked with key process parameters such as the MOI, time of infection, and time of harvest, which should be optimized on a product-specific basis [58]. For industrialscale production, it may be better to focus on process stability, which ensures high product quality and homogeneity, even if this means accepting some drawbacks. We used an HFM to demonstrate the shear sensitivity of infected insect cells, but process control and monitoring is rather limited in this type of reactor. Therefore, cell lysis and the resulting release of proteases cannot be predicted, and the product quality may be more heterogeneous due to gradients along the length of the membrane fibers. Wave bioreactors are characterized by low shear stress but the size limitations make them unsuitable for industrialscale processes [27]. STRs cause more shear stress but our results suggest that the damage can be limited by a careful choice of aeration strategy and the inclusion of cell-protecting agents such as Pluronic. Therefore, STRs remain the most suitable bioreactor type for the scale-up of BEVS processes for the production of high-quality recombinant proteins.

List of abbreviations and symbols

и	specific area of the gas phase
BEVS	baculovirus expression vector system
$C_{_{ m D}}$	stirrer-specific dissipation coefficient
d	diameter
$d_{_{32}}$	Sauter diameter
$d_{_{ m B}}$	bubble diameter
$d_{\rm c}$	dell diameter
$d_{_{ m sh}}$	diameter of shaker flask
$d_{_{ m st}}$	stirrer diameter
$d_{_{ m R}}$	reactor diameter
ECS	extra-capillary space
HFM	hollow fiber module
$h_{_{ m L}}$	height of fluid
$h_{_{ m V}}$	height of volume
$k_{\rm d}$	specific death rate
$k_{_{ m L}}$	transport coefficient in the liquid
$k_{_{ m La}}$	oxygen transfer coefficient
MOI	multiplicity of infection
Ne'	modified Newton number
Q	aeration rate
qO_{2}	oxygen uptake rate
Re	Reynolds number
STR	stirred tank reactor
$V_{_{ m K}}$	volume in the wake of rising bubbles
$V_{_{ m L}}$	filling volume
$W_{ m tip}$	stirrer tip speed
X	biomass concentration
ε	average energy dissipation per mass
$\varepsilon_{\mathrm{max}}$	maximal energy dissipation per mass
η	eddy scale
ν	viscosity

Acknowledgments: We thank the Hessen State Ministry of Higher Education, Research and the Arts for financial support within the Hessen initiative for scientific and economic excellence (LOEWE-Program). The authors acknowledge Dr. Richard M. Twyman for editing the paper.

References

- 1. Grace TD. Establishment of four strains of cells from insect tissues grown in vitro. Nature 1962;195:788-9.
- 2. Lynn DE. Novel techniques to establish new insect cell lines. In Vitro Cell Dev Biol Anim 2001;37:319.
- 3. Lynn DE, Harrison RL. Available Lepidopteran insect cell lines. In: Murhammer DW, editor. Baculovirus and insect cell expression protocols. New York, NY: Humana Press, 2016:119-42.
- 4. Smith GE, Summers MD, Fraser MJ. Production of human beta interferon in insect cells infected with a baculovirus expression vector. Mol Cell Biol 1983;3:2156-65.
- 5. McCarroll L, King LA. Stable insect cell cultures for recombinant protein production. Curr Opin Biotechnol 1997;8:590-4.
- 6. Dyring C. Optimising the Drosophila S2 expression system for production of therapeutic vaccines. BioProcess J 2011;10:28-35.

- 7. Zitzmann J, Weidner T, Czermak P. Optimized expression of the antimicrobial protein gloverin from Galleria mellonella using stably transformed Drosophila melanogaster S2 cells. Cytotechnology 2017;69:371-69.
- 8. Wilde M, Klausberger M, Palmberger D, Ernst W, Grabherr R. Tnao38, High Five and Sf9 – evaluation of host-virus interactions in three different insect cell lines: baculovirus production and recombinant protein expression. Biotechnol Lett 2014;36:743-9.
- 9. van Oers MM, Pijlman GP, Vlak JM. Thirty years of baculovirusinsect cell protein expression: from dark horse to mainstream technology. J Gen Virol 2015;96:6-23.
- 10. Airenne KJ, Hu Y-C, Kost TA, Smith RH, Kotin RM, Ono C, et al. Baculovirus: an insect-derived vector for diverse gene transfer applications. Mol Ther 2013;21:739-49.
- 11. Monteiro F, Bernal V, Saelens X, Lozano AB, Bernal C, Sevilla A, et al. Metabolic profiling of insect cell lines: unveiling cell line determinants behind system's productivity. Biotechnol Bioeng 2014;111:816-28.
- 12. Bernal V, Carinhas N, Yokomizo AY, Carrondo MJ, Alves PM. Cell density effect in the baculovirus-insect cells system: a quantitative analysis of energetic metabolism. Biotechnol Bioeng 2009;104:162-80.
- 13. Monteiro F, Carinhas N, Carrondo MJ, Bernal V, Alves PM. Toward system-level understanding of baculovirus-host cell interactions: from molecular fundamental studies to large-scale proteomics approaches. Front Microbiol 2012;3;391.
- 14. Carpentier DC, Griffiths CM, King LA. The baculovirus P10 protein of Autographa californica nucleopolyhedrovirus forms two distinct cytoskeletal-like structures and associates with polyhedral occlusion bodies during infection. Virology 2008;371:278-91.
- 15. Ohkawa T, Volkman LE, Welch MD. Actin-based motility drives baculovirus transit to the nucleus and cell surface. J Cell Biol 2010;190:187-95.
- 16. Ustun-Aytekin O, Gurhan ID, Ohura K, Imai T, Ongen G. Monitoring of the effects of transfection with baculovirus on Sf9 cell line and expression of human dipeptidyl peptidase IV. Cytotechnology 2014;66:159-68.
- 17. Xing Z, Kenty BM, Li ZJ, Lee SS. Scale-up analysis for a CHO cell culture process in large-scale bioreactors. Biotechnol Bioeng 2009;103:733-46.
- 18. Ducommun P, Ruffieux P-A, Furter M-P, Marison I, Stockar UV. A new method for on-line measurement of the volumetric oxygen uptake rate in membrane aerated animal cell cultures. J Biotechnol 2000;78:139-47.
- 19. Backer MP, Metzger LS, Slaber PL, Nevitt KL, Boder GB. Largescale production of monoclonal antibodies in suspension culture. Biotechnol Bioeng 1988;32:993-1000.
- 20. Zhou W, Hu WS. On-line characterization of a hybridoma cell culture process. Biotechnol Bioeng 1994;44:170-7.
- 21. Yoon SJ, Konstantinov KB. Continuous, real-time monitoring of the oxygen uptake rate (OUR) in animal cell bioreactors. Biotechnol Bioeng 1994;44:983-90.
- 22. Wong TK, Nielsen KL, Greenfield PF, Reid S. Relationship between oxygen uptake rate and time of infection of Sf9 insect cells infected with a recombinant baculovirus. Cytotechnology 1994;15:157-67.
- 23. Hensler W, Agathos S. Evaluation of monitoring approaches and effects of culture conditions on recombinant protein production in baculovirus-infected insect cells. Cytotechnology 1994;15:177-86.

- 24. Palomares LA, López S, Ramírez OT. Utilization of oxygen uptake rate to assess the role of glucose and glutamine in the metabolism of infected insect cell cultures. Biochem Eng J 2004;19:87-93.
- 25. Cowger NL, O'Connor KC, Bivins JE. Influence of simulated microgravity on the longevity of insect-cell culture. Enzyme Microb Technol 1997;20:326-32.
- 26. Ikonomou L, Schneider Y-J, Agathos SN. Insect cell culture for industrial production of recombinant proteins. Appl Microbiol Biotechnol 2003;62:1-20.
- 27. Contreras-Gómez A, Sánchez-Mirón A, García-Camacho F, Chisti Y, Molina-Grima E. Protein production using the baculovirusinsect cell expression system. Biotechnol Prog 2014;30:1-18.
- 28. Roldão A, Cox M, Alves P, Carrondo M, Vicente T. Industrial large scale of suspension culture of insect cells. In: Schmidhalter DR. Meyer H-P, editors. Industrial scale suspension culture of living cells. Weinheim, Germany: Wiley Blackwell, 2014:348-89.
- 29. Henzler H-J. Particle stress in bioreactors. In: Schügerl K, Kretzmer G, Henzler HJ, MacLoughlin PE, Malone DM, Schumann W, Shamlou PA, Yim SS, editors. Influence of stress on cell growth and product formation. Berlin, Heidelberg: Springer Berlin Heidelberg, 2000:35-82.
- 30. Kolmogorov A. The local structure of turbulence in incompressible viscous fluid for very large Reynold's numbers. C.R. Acad. Sci. U.S.S.R., 1941;301-5.
- 31. Godoy-Silva R, Berdugo C, Chalmers JJ, Flickinger MC. Aeration, mixing, and hydrodynamics, animal cell bioreactors. In: Encyclopedia of industrial biotechnology. John Wiley and Sons, Inc., 2010.
- 32. Liepe F, Sperling R, Jembere S. Rührwerke: Theoretische Grundlagen, Auslegung und Bewertung: Köthen, Fachhochschule, 1998.
- 33. Garcia-Briones MA, Chalmers JJ. Flow parameters associated with hydrodynamic cell injury. Biotechnol Bioeng 1994;44:1089-98.
- 34. Chisti Y. Animal-cell damage in sparged bioreactors. Trends Biotechnol 2000;18:420-32.
- 35. Tramper J, Smit D, Straatman J, Vlak JM. Bubble-column design for growth of fragile insect cells. Bioprocess Eng 1988;3:37-41.
- 36. Tramper J, Williams JB, Joustra D, Vlak JM. Shear sensitivity of insect cells in suspension. Enzyme Microb Technol 1986;8:33-6.
- 37. Boulton-Stone JM, Blake JR. Gas bubbles bursting at a free surface. J Fluid Mech 1993;254:437.
- 38. Murhammer DW. Pluronic polyols, cell protection. In: Flickinger MC, editor. Encyclopedia of bioprocess technology, fermentation, biocatalysis, and bioseparation. New York, NY: Wiley, 1999.
- 39. Nienow AW. Impeller selection for animal cell culture. In: Flickinger MC, editor. Encyclopedia of industrial biotechnology, bioprocess, bioseparation, and cell technology. Hoboken, NJ: Wiley, 2010.
- 40. Chalmers JJ, Bavarian F. Microscopic visualization of insect cell-bubble interactions. II: The bubble film and bubble rupture. Biotechnol Prog 1991;7:151-8.
- 41. Garcia-Briones M, Chalmers JJ. Cell-bubble interactions. Ann NY Acad Sci 1992;665:219-29.
- 42. Chattopadhyay D, Rathman JF, Chalmers JJ. The protective effect of specific medium additives with respect to bubble rupture. Biotechnol Bioeng 1995;45:473-80.
- 43. Ma N, Chalmers JJ, Aunins JG, Zhou W, Xie L. Quantitative studies of cell-bubble interactions and cell damage at different pluronic F-68 and cell concentrations. Biotechnol Prog 2004;20:1183-91.

- 44. Eibl R, Kaiser S, Lombriser R, Eibl D. Disposable bioreactors: the current state-of-the-art and recommended applications in biotechnology. Appl Microbiol Biotechnol 2010;86:41-9.
- 45. Marks DM. Equipment design considerations for large scale cell culture. Cytotechnology 2003;42:21-33.
- 46. Nehring D, Czermak P, Vorlop J, Lubben H. Experimental study of a ceramic microsparging aeration system in a pilot-scale animal cell culture. Biotechnol Prog 2004;20:1710-7.
- 47. Czermak P, Pörtner R, Brix A. Special engineering aspects. In: Martin F, Wilfried W, editors. Cell and tissue reaction engineering: with a contribution. Berlin, Heidelberg: Springer Berlin Heidelberg, 2009:83-172.
- 48. Druzinec D, Salzig D, Kraume M, Czermak P. Micro-bubble aeration in turbulent stirred bioreactors: coalescence behavior in Pluronic F68 containing cell culture media. Chem Eng Sci 2015:126:160-8.
- 49. Reed L, Muench H. A simple method of estimating fifty per cent endpoints. Am J Epidemiol 1938;27:493-7.
- 50. Sprick G, Zitzmann J, Weidner T, Czermak P, editors. Cell culture: process optimization for recombinant protein expression in insect cells. Rijeka, Croatia: InTech Europe, 2017.
- 51. O'Reilly DR, Miller LK, Luckow VA. The Baculovirus expression vectors: a laboratory manual. New York: Oxford University Press,
- 52. Peter CP, Suzuki Y, Büchs J. Hydromechanical stress in shake flasks: correlation for the maximum local energy dissipation rate. Biotechnol Bioeng 2006;93:1164-76.

- 53. Büchs J, Maier U, Milbradt C, Zoels B. Power consumption in shaking flasks on rotary shaking machines: II. Nondimensional description of specific power consumption and flow regimes in unbaffled flasks at elevated liquid viscosity. Biotechnol Bioeng 2000;68:594-601.
- 54. de Almeida AF, de Macedo GR, Chan LC, da Silva Pedrini MR. Kinetic analysis of in vitro production of wild-type Spodoptera frugiperda nucleopolyhedrovirus. Braz Arch Biol Technol 2010:53:285-91.
- 55. Rhiel M, Mitchell-Logean CM, Murhammer DW. Comparison of Trichoplusia ni BTI-Tn-5B1-4 (High Five(R)) and Spodoptera frugiperda Sf-9 insect cell line metabolism in suspension cultures. Biotechnol Bioeng 1997;55:909.
- 56. Weber W, Weber E, Geisse S, Memmert K. Optimisation of protein expression and establishment of the wave bioreactor for Baculovirus/insect cell culture. Cytotechnology 2002;38:77-85.
- 57. Yang P, Teo W-K, Ting Y-P. Design and performance study of a novel immobilized hollow fiber membrane bioreactor. Bioresour Technol 2006;97:39-46.
- 58. Drugmand J-C, Schneider Y-J, Agathos SN. Insect cells as factories for biomanufacturing. Biotechnol Adv 2012;30:1140-57.
- 59. Clem RJ. Baculoviruses and apoptosis: the good, the bad, and the ugly. Cell Death Differ 2001;8:137-43.
- 60. Clem RJ, Fechheimer M, Miller LK. Prevention of apoptosis by a Baculovirus gene during infection of insect cells. Science 1991;5036:1388-90.